COMPDYN 2011
3rd ECCOMAS Thematic Conference on
Computational Methods in Structural Dynamics and Earthquake Engineering
M. Papadrakakis, M. Fragiadakis, V. Plevris (eds.)
Corfu, Greece, 25-28 May 2011

ENHANCED 3D FIBER BEAM-COLUMN ELEMENT WITH WARPING DISPLACEMENTS

V. Le Corvec[1], F.C. Filippou[2]

[1] University of California, Berkeley- Dept of Civil and Environmental Engineering
760 Davis Hall - 94720 Berkeley CA, USA
e-mail: lecorvec@berkeley.edu

[2] University of California, Berkeley- Dept of Civil and Environmental Engineering
760 Davis Hall - 94720 Berkeley CA, USA
e-mail: filippou@berkeley.edu

Keywords: fiber beam, mixed formulation, shear, torsion, shear lag

Abstract. *Beam elements are commonly used in the analysis of steel and reinforced concrete structures in earthquake engineering practice. These elements reproduce the global behavior of these structures at a reasonable computational cost. For this type of analysis the force-based fiber beam element has proven an excellent compromise between accuracy and computational cost for the simulation of the inelastic response of structural models of significant size. Recent studies have proposed extensions of the model to account for the effect of shear and torsion under fixed shear strain or stress distributions. These assumptions suffer from shortcomings for the representation of the coupling between shear and torsion, and are not suitable for the representation of local stress and strain distributions at critical sections. To describe such complex stress states, shell finite element models are often used with a significant increase in computational cost. This paper presents the mixed formulation of an enhanced 3d fiber beam element that represents accurately the global and local response of structural members under axial force, flexure, shear and torsion interaction. The proposed 3d fiber beam element determines the shear strain distribution at a section from the satisfaction of local equilibrium equations with the section warping displacements as local parameters. Unlike existing models, the coupling between sections is taken in account. Hence the enhanced fiber beam-column is able to capture the local effects due to constrained warping of the section, such as the flange shear lag effect. The model is also capable of representing accurately the maximum local stress at element boundaries, and of simulating the torsional response of beams under warping constraints.*

The element is validated with several examples involving inelastic response of steel members under high shear force, such as shear links. The simulations are conducted under monotonic and cyclic load conditions for specimens with wide flange and box sections. The accuracy and computational efficiency of the proposed element is demonstrated by comparing the results with experimental values and with local response estimates of shell finite element models.

1 INTRODUCTION

Nonlinear analysis is used increasingly for the evaluation of structures under extreme loading conditions. This type of loads induces high inelastic strains at critical sections and large node displacements. Recent studies have shown that the corotational formulation is a suitable framework for the description of large displacements allowing the nonlinear material response of the basic element to be limited to small deformations. For frame elements the force-based fiber beam element by Ciampi and Carlesimo [4] with its subsequent embedment in a consistent variational framework by Taylor [11] and Lee [7] has proven an excellent choice for describing the interaction between axial force and flexure under inelastic material response.
Recently, research interest has focused on the extension of the force-based beam element to the effect of shear and torsion. In older structures and short span elements the shear affects the failure mode and the member capacity. The first formulation of a beam element with shear was based on Timonshenko beam theory with the assumption of a constant shear stress distribution over the cross-section [12]. Subsequent models by A. Saritas [10], N. Gregori [5] and A. Papachristidis [9], postulate a strain or stress field distribution based on the analytical result for a homogeneous section. These models were used to simulate the inelastic response of shear links and shear walls with success. However, the assumption of a fixed shear distribution is not justified when inelastic deformations spread through the section and render the response inhomogeneous. The model of J.M. Bairan [1] and S. Mohr [8] overcomes this limitation with the addition of degrees of the freedom at the section level to represent the shear distribution while also accounting for section warping. Equations of local equilibrium are used to determine the response parameters at these degrees of freedom.
The model of A.Saritas [10] is limited to 2d applications, whereas the element proposed by N. Gregori [5] and A. Papachristidis [9] apply to 3d response without, however, accounting for the shear distribution due to torsion and the effect of warping. The model of J.M. Bairan [1] accounts for section warping and is thus able to represent the torsional response with accuracy. The model also accounts for the in-plane section deformation, which increases computational cost significantly.
Even though existing models account for a variable shear distribution and section warping, the interaction between sections of the beam element is not directly taken into account. In particular the effect of warping on axial deformation is neglected resulting in the incorrect representation of the local response near boundaries and other important local response phenomena such as shear-lag [13]. While neglecting this effect and decoupling the response of different beam sections has the advantage of maintaining the number of element degrees of freedom and reducing the element computational cost, the inability of representing the local stresses under warping constraints and at element boundaries is a serious limitation.
The proposed 3d enhanced fiber beam element model sets out to address some limitations of earlier formulations by allowing for arbitrary section warping under shear and torsion and by including the effect of boundaries on the warping distribution. This objective is met first with the introduction of warping degrees of freedom at each section, and secondly by imposing equilibrium on the entire element, so as to account for section interaction and thus incorporate the effect of boundary conditions. For simplicity only out-of-plane section displacements are represented by assuming that the section is rigid in its plane.
The paper presents a brief description of the theory of the proposed 3d enhanced fiber beam element and concludes with a few examples that demonstrate its capability for representing the shear stress distribution under combined loadings and the shear lag effect. In these examples

the response of structural model with the proposed element is compared with the response of the model with shell elements, thus permitting for the accurate comparison of the global as well as the local response.

2 BEAM DESCRIPTION

This section presents a brief derivation of the enhanced 3d beam element. The element is formulated in a system without rigid body modes, which are removed with the corotational formulation.
The element degrees of freedom consist of local degrees of freedom $\mathbf{u}_{IJ}$ and of warping degrees of freedom $\mathbf{u}^w_{IJ}$. The warping degrees of freedom describe the out-of-plane displacements of

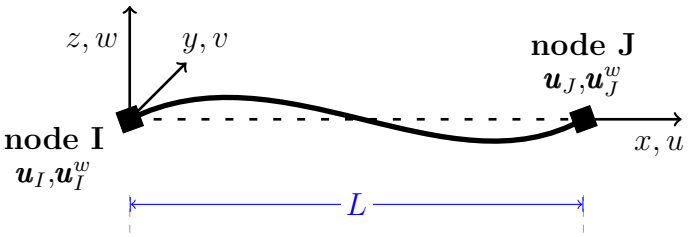

Figure 1: Basic element kinematics

the section. The number of these degrees of freedom for each section is n_w. These are local degrees of freedom associated with local equilibrium equations. To satisfy displacement compatibility between adjacent elements, the warping displacements of the end sections are retained as element variables.

$$\mathbf{u}^w_{IJ} = \begin{bmatrix} \mathbf{u}^w_I & \mathbf{u}^w_J \end{bmatrix} \tag{1}$$

In the local reference system the element deformations are denoted by $\mathbf{v}$ and consist of the axial deformation, of the rotations θ_y and θ_z at the element ends, and of the angle of twist ϕ. The associated forces $\mathbf{q}$ are the axial force, the bending moments about the y and z axis, and the torsional moment. The deformations are related to the local displacements with the compatibility matrix $\mathbf{a}_g$:

$$\mathbf{v} = \mathbf{a}_g \mathbf{u}_{IJ} \tag{2}$$

2.1 Section Kinematics

The displacements of any point (y,z) of a section, defined by its x along the element axis, are decomposed as follows:

$$\mathbf{u}_{total} = \mathbf{u}^r + \mathbf{u}^w \tag{3}$$

The rigid displacement of the section is denoted by $\mathbf{u}^r$ and is expressed in terms of the cross-section generalized displacements

$$\mathbf{u}(x) = \begin{bmatrix} u & v & w & \theta_z & \theta_y & \phi \end{bmatrix}^T (x) \tag{4}$$

The warping displacements $\mathbf{u}^w(x,y,z)$ are defined everywhere in the beam element by interpolation functions

$$\mathbf{u}^w(x,y,z) = \sum_{ij} M_i(x) N_j(y,z) \mathbf{u}^w(x_i, y_j, z_j) \tag{5}$$

In contrast to the formulation by J.M. Bairan [1], only the axial component of the warping displacement is taken into account by neglecting the in-plane section deformation.

The warping displacements are orthogonal to the section rigid body displacements $\mathbf{u}^r$. This condition is enforced by removing the rigid body modes from the displacements $\mathbf{u}^w$ with the use of a projection matrix. The details of this matrix are not presented here for the sake of brevity.

The displacement of any material point (y,z) of the cross section at position x along the axis is given by

$$u_x(x,y,z) = u(x) - y\theta_z(x) + z\theta_y(x) + u^w(x,y,z) \tag{6}$$
$$u_y(x,y,z) = v(x) - z\phi(x) \tag{7}$$
$$u_z(x,y,z) = w(x) + y\phi(x) \tag{8}$$

The strains are derived from the definition of the displacements and are expressed in the compact form:

$$\boldsymbol{\epsilon}(\mathbf{u}^r, \mathbf{u}^w) = \begin{bmatrix} \epsilon_{xx} \\ 2\epsilon_{xy} \\ 2\epsilon_{xz} \end{bmatrix} = \begin{bmatrix} 1 & -y & 0 & 0 & z & 0 \\ 0 & 0 & 1 & -z & 0 & 0 \\ 0 & 0 & 0 & y & 0 & 1 \end{bmatrix} \begin{bmatrix} u' \\ \theta_z' \\ v' - \theta_z \\ \phi' \\ \theta_y' \\ w' - \theta_y \end{bmatrix} + \begin{bmatrix} \epsilon_{xx}(\mathbf{u}^w) \\ 2\epsilon_{xy}(\mathbf{u}^w) \\ 2\epsilon_{xz}(\mathbf{u}^w) \end{bmatrix} \tag{9}$$

$$= \mathbf{a}_s \mathbf{e}(\mathbf{u}) + \boldsymbol{\epsilon}(\mathbf{u}^w) \tag{10}$$

where the notation $'$ denotes the derivative of the variable with respect to coordinate x.
The notation $\mathbf{e}$ for the generalized section deformations is introduced

$$\mathbf{e} = \begin{bmatrix} \epsilon_0 & \kappa_z & \gamma_y & \kappa_x & \kappa_y & \gamma_z \end{bmatrix}^T \tag{11}$$

where ϵ_0 is the axial strain, κ_z and κ_y the two curvatures and γ_y and γ_z the shear strains.
According to equation (10), the warping displacement contributes to the axial strain and to the shear strain. This fact is critical in the description of the effect of boundary conditions and the additional stresses due to warping constraints.

2.2 Variational principle

The element formulation is based on the Hu-Washizu variational principle [7]. The potential function of displacements $\mathbf{u}$ and $\mathbf{u}^w$, section deformations $\mathbf{e}$ and stresses $\boldsymbol{\sigma}$ is defined over the element volume V by

$$\Pi(\mathbf{u}, \mathbf{u}^w, \mathbf{e}, \boldsymbol{\sigma}) = \int_V \boldsymbol{\sigma}^T (\mathbf{a}_s \mathbf{e}(\mathbf{u}) - \mathbf{a}_s \mathbf{e})\, dV + \int_V W(\mathbf{e}, \mathbf{u}^w) dV + \Pi_{ext}(\mathbf{u}_{IJ}, \mathbf{u}^w_{IJ}) \tag{12}$$

where W is the internal potential energy. In the form of (12), the element formulation is mixed: the warping strain is derived from the warping displacements, while the section deformations

are imposed in weak form.
The external load is defined by

$$\Pi_{ext} = -\mathbf{u}_{IJ}^T \bar{\mathbf{p}} - \mathbf{u}_{IJ}^{wT} \bar{\mathbf{p}}^w \tag{13}$$

The forces $\bar{\mathbf{p}}$ and $\bar{\mathbf{p}}^w$ are the applied forces at the end nodes of the element. If the end sections are free to warp, the applied warping force is $\bar{\mathbf{p}}^w = \mathbf{0}$. Otherwise, warping displacements $\mathbf{u}_{IJ}^w$ are imposed. The case of element loading is not included for the sake of simplicity.

The variation of potential Π leads to the definition of the associative section forces by integration over the cross-section area A:

$$\mathbf{s} = \int_A \mathbf{a}_s^T \boldsymbol{\sigma} dA \ , \ s_x^{wj} = \int_A N_j \sigma_{xx} dA \ , \ s_{yz}^{wj} = \int_A \frac{\partial N_j}{\partial y}\sigma_{xy} + \frac{\partial N_j}{\partial z}\sigma_{xz} dA \tag{14}$$

By minimization of the potential Π, we obtain a set of equations:

$$\bar{\mathbf{p}} = \mathbf{a}_g \mathbf{q} \tag{15}$$
$$\mathbf{s}_i = \mathbf{b}(x_i)\mathbf{q} \tag{16}$$
$$\mathbf{v} = \int_0^L \mathbf{b}^T \mathbf{e} dx \tag{17}$$
$$\boldsymbol{\sigma} = \frac{\partial W}{\partial \boldsymbol{\epsilon}} \tag{18}$$
$$p_i^{wj} = \int_0^L \frac{\partial M_i}{\partial x} s_x^{wj} dx + \int_0^L M_i s_{yz}^{wj} dx \tag{19}$$

where $\mathbf{b}$ is a linear interpolation matrix given by

$$\mathbf{b}(x) = \begin{bmatrix} 1 & 0 & 0 & 0 & 0 & 0 \\ 0 & x/L & 1-x/L & 0 & 0 & 0 \\ 0 & 1/L & 1/L & 0 & 0 & 0 \\ 0 & 0 & 0 & 1 & 0 & 0 \\ 0 & 0 & 0 & 0 & x/L & 1-x/L \\ 0 & 0 & 0 & 0 & 1/L & 1/L \end{bmatrix} \tag{20}$$

The first four equations correspond to the mixed formulation equations for the beam: the equilibrium equations (15-16), the compatibility equation (17) and the constitutive law (18). The additional equations (19) correspond to the equilibrium conditions that need to be satisfied by the warping section forces $\mathbf{s}_x^w$ and $\mathbf{s}_{yz}^w$. These equilibrium equations are imposed at each section x_i with warping displacements $\mathbf{u}^w(x_i, ., .)$ as the unknowns (5). The section deformations and the warping displacements are determined during the element state determination by satisfying the equilibrium and compatibility equations.
The tangent stiffness associated with the set of equations (15-19) ensures optimal convergence of the element state determination algorithm.

2.3 Interpolations

The section warping is described by warping parameters denoted with $\mathbf{u}_{ij}^w$. The warping is then described over the section with the functions $N_j(y, z)$ in equation (5). With Lagrange polynomials for the functions N_j the warping parameters $\mathbf{u}_{ij}^w$ can be interpreted as local warping

values. This approach differs from the fixed strain distribution assumed in earlier studies [10]. The enforcement of the warping equilibrium equations results in an accurate strain distribution. This formulation can be applied to any section geometry and does not require a shear correction factor, as is the case with earlier studies [10] and [9]. To reduce the number of warping parameters, advantage can be taken of the geometric characteristics of the section, such as symmetry and double-symmetry, in the choice of interpolation functions $N_j(y, z)$, as proposed in the report by Setec-Tpi [6].
The determination of the warping distribution over the element length is accomplished with the interpolation functions $M(x)$. For constrained warping, the choice of interpolation functions is critical. Under linear elastic response, the analytical solution consists of an exponential distribution of warping displacements along the element axis. Among the different choices for interpolation functions M are exponential functions, Lagrange polynomials, and quadratic spline functions. In the examples of the following section Lagrange polynomials are used.

3 EXAMPLES

The examples presented below demonstrate the capabilities of the enhanced 3d element. The element is tested on two shear links. Its response is compared to the response of the beam element by A.Saritas[10], which is extended to 3d with the assumption of a fixed shear strain distribution. The link response is also compared with the response of a model consisting of MITC shell elements [2]. The nonlinear material response of structural steel is described with the J2 plasticity model. The studies compare the global force-displacement response as well as the local stress distributions with focus on the axial stress σ_{xx} associated with the warping constraints.
The test configuration for the two shear links is shown in figure 2. Warping is assumed to be constrained at both ends. To demonstrate the coupling between shear and torsion, the element is allowed to twist at one end when the shear force is applied with an eccentricity. The shear link is modeled with one 3d beam element with 5 Gauss-Lobatto integration points along its axis.

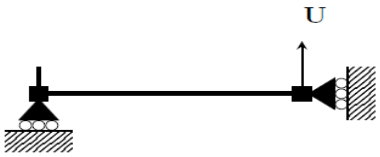

Figure 2: Shear Link Configuration

3.1 Example 1

The cross-section of the shear link is shown in figure 3. The length of the shear link is L= 456 mm. This example is part of the experimental campaign by Berman and Bruneau [3]. The analysis with beam elements is compared with the experimental results and the results with a shell model by limiting attention to the first three load cycles. The enhanced 3d beam element uses n_w=12 parameters in each section to describe the section warping. Figure 4 shows that the response of the three models is very close in terms of the shear reaction force for an imposed vertical displacement (or shear link rotation) and agrees very well with experimental measurements.
The local stress results are plotted for a link rotation $\gamma = U/L = 0.006$ in the transition to

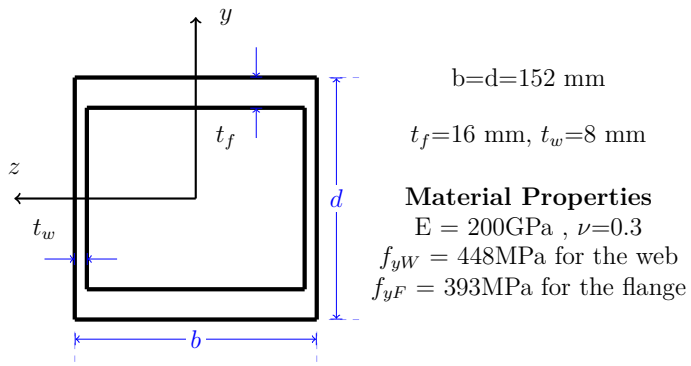

Figure 3: Cross section properties

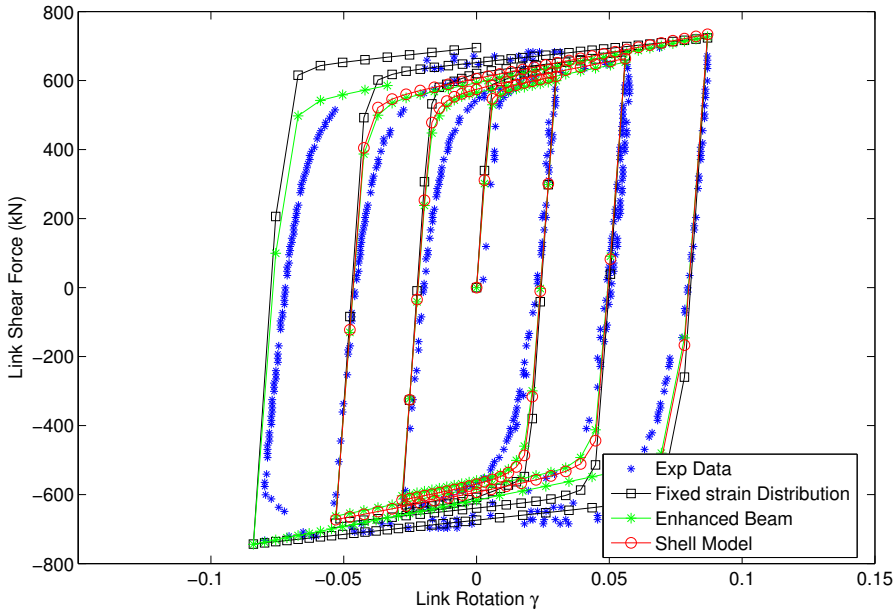

Figure 4: Shear link rotation vs. Shear Force

the plastic range. The figures 5 and 6 present the shear stresses of the middle section of the element, where warping is free. The results confirm that the enhanced 3d beam reproduces the shear stress distribution postulated by the fixed shear strain assumption of A. Saritas [10]. The distribution of the shear stresses σ_{xz} in the upper flange is also represented accurately.

The shear lag effect takes place at the boundary of the beam and at the load application points. At this boundary section, the warping constraint creates additional axial stresses. The comparison of the axial stresses in the web and in the flange is presented in figures 7 and 8. The enhanced 3d beam element gives a correct estimation of the maximum axial stress in the web, which is 30% higher than the value predicted by the beam with a fixed shear strain distribution.

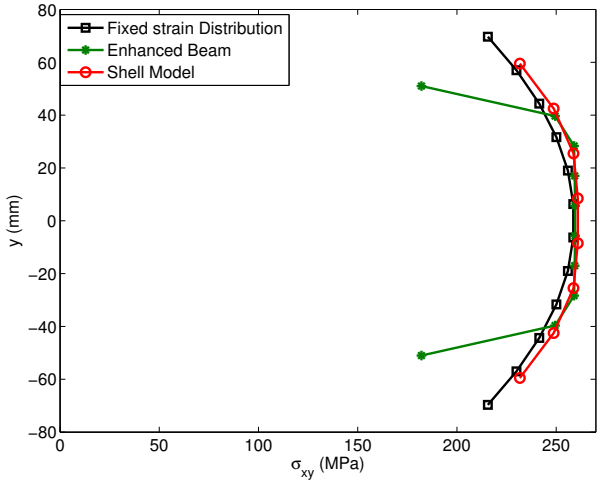

Figure 5: Shear stresses in the left web

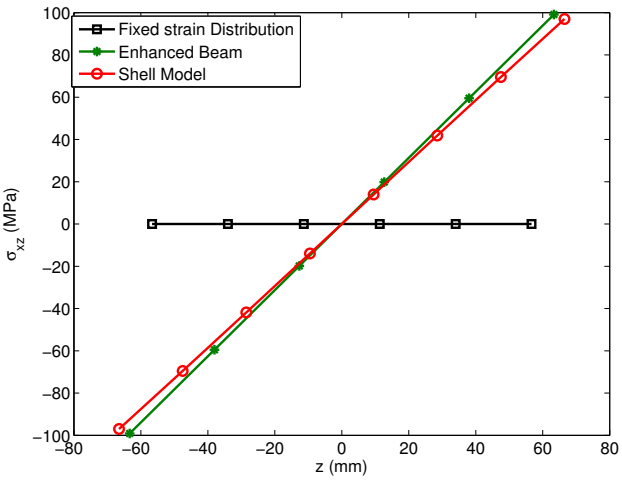

Figure 6: Shear stresses in the lower flange

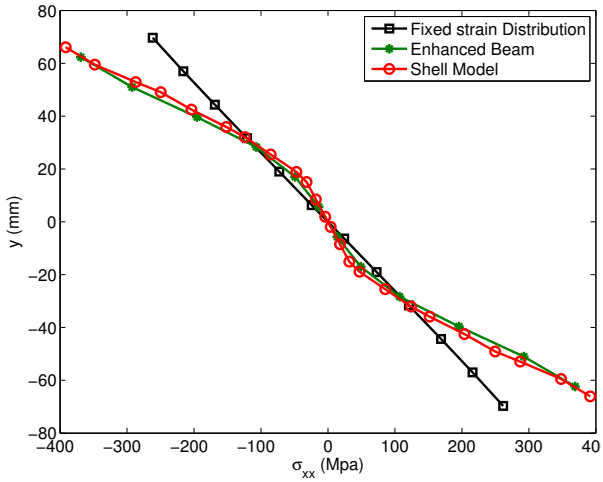

Figure 7: Axial stresses in the web

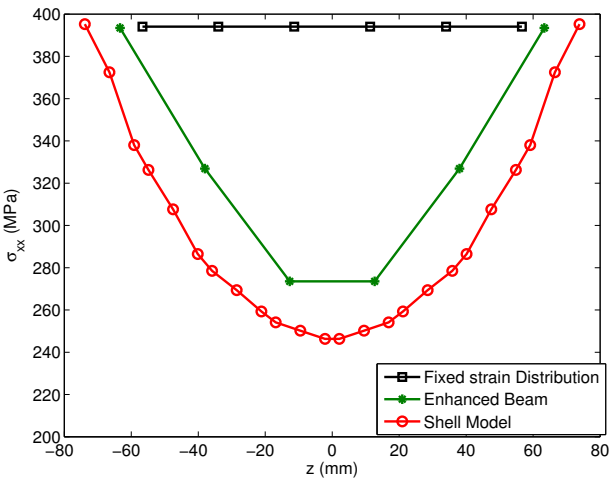

Figure 8: Axial stresses in the lower flange

3.2 Example 2

The dimensions of the I cross-section of the shear link are presented in figure 9. The length of the shear link is L =28in. The steel material is described by a generalized J2 plasticity Model, as presented in [10].

A shear force is applied on the shear link. To model the effect of torsion, the force is applied with an eccentricity of e_c =2 in from the centroid to create a torsional moment proportional to the shear force. The enhanced 3d beam describes the section warping with n_w=28 parameters. The figures 10 and 11 present the force-displacement response of the shear link: the shear force is plotted against the vertical displacement and the torsion force against the angle of twist ϕ. The enhanced beam model is able to represent with accuracy the lateral and torsional stiffness as well as the yielding force. In comparison, the beam with a fixed shear strain distribution cannot represent the exact elastic torsional stiffness, since warping is not taken into account. The interaction between shear and torsion is demonstrated in 10.

In addition to the global response, the proposed element describes with accuracy the local

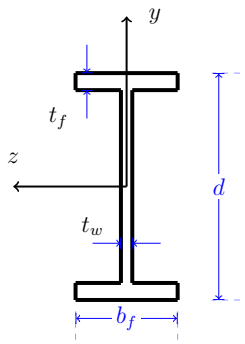

d=17.88in
b_f=5.985 in
t_f=0.521 in, t_w= 0.314 in

Material Properties
for the web E_W= 28300ksi , ν=0.3
f_{yW} = 39.5ksi f_{uW}= 60.1ksi
for the flange E_F= 28000ksi , ν=0.3
f_{yF} = 35ksi f_{uF}= 58.5ksi

Figure 9: Cross section properties

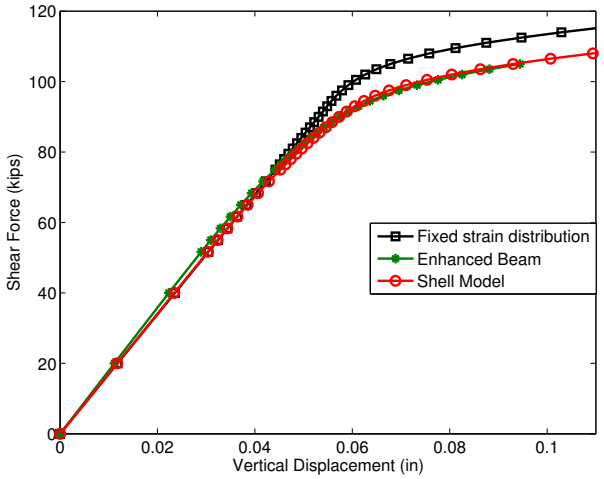

Figure 10: Shear Force vs. Vertical Displacement

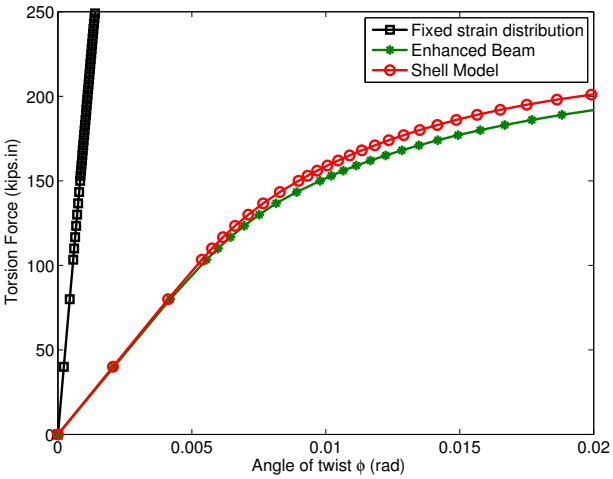

Figure 11: Torsion Force vs. Twist Angle

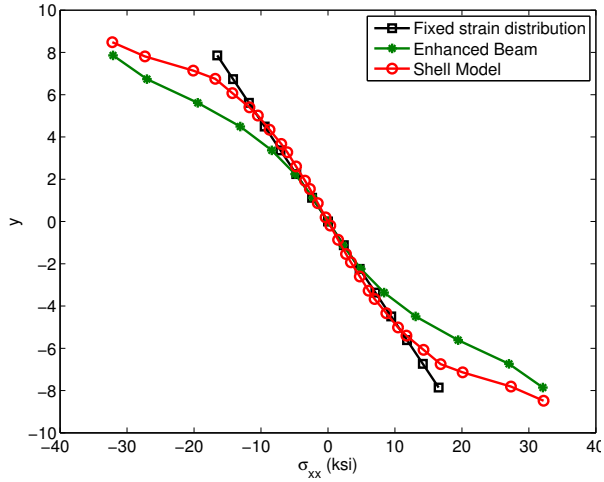

Figure 12: Axial stresses in the web

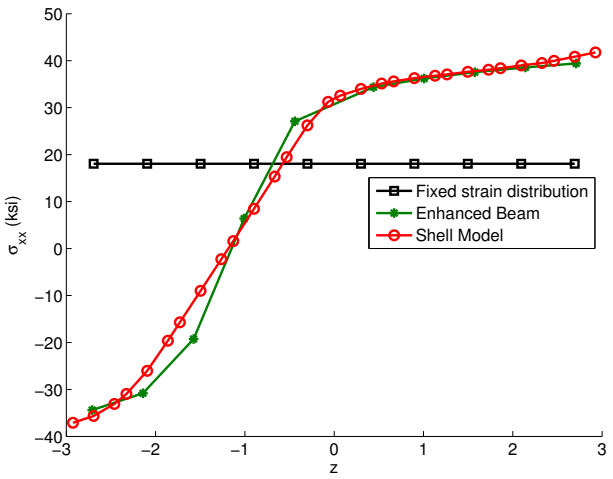

Figure 13: Axial stresses in the lower flange

response in the plastic range. For a shear force of 88.5 kips, the axial stresses at the boundary section are plotted for the web 12 and the lower flange 13 respectively.

4 CONCLUSIONS

The paper presents a 3d enhanced fiber beam element formulation that includes warping degrees of freedom so as to represent the effect of shear and torsion. No shear correction factor is required with the shear strain distribution determined directly from the section warping. The element is capable of representing accurately the local response of beams under different constraints for which a shell element is usually required. It is also capable of describing accurately the shear lag effect at a significantly lower computational cost than a shell model.
A few examples demonstrate the capabilities of the element for simulating inelastic response of steel structures under flexure, shear and torsion. Studies are under way to extend the element formulation to reinforced concrete frames, for which existing studies demonstrate the importance of shear modeling [8]. Further studies to optimize the element performance for earthquake engineering applications by reducing the number of warping degrees of freedom are under way.

5 ACKNOWLEDGEMENTS

The present work was sponsored by Setec TPI. The authors are grateful for the financial support and thank Dr Michel Kahan and Xavier Cespedes for their support and encouragement during the course of the study. The authors are also grateful for the exchange of information about the problem of torsion with warping constraints with Xavier Cespedes and his team. (www.tpi.setec.fr)

REFERENCES

[1] J M. Bairan, A non-linear totally-coupled model for RC sections under 3D bending, shear, torsion and axial loading. *PhD thesis* Technical University of Catalonia. Barcelona, 2005.

[2] K.-J. Bathe, E.N Dvorkin, A formulation of general shell elements- The use of mixed interpolation of tensorial components. *International Journal of Numerical Methods in Engineering* **22**, 697-722,1986.

[3] J.W. Berman, M. Bruneau, Experimental and analytical investigation of tubular links for eccentrically braced frames. *Engineering Structures* **8**, 1929–1938, 2007.

[4] V. Ciampi, L. Carlesimo, A Nonlinear Beam Element for Seismic Analysis of Structures. *8th European Conference on Earthquake Engineering, Lisbon, Laboratorio Nacional de Engenharia Civil* 1986

[5] J. N. Gregori, P. M. Sosa, M.A. F. Prada, F. C. Filippou, A 3D numerical model for reinforced and prestressed concrete elements subjected to combined axial, bending, shear and torsion loading. *Engineering Structures* **29**, 3404–3419, 2007.

[6] K. Ferradi, Etude du gauchissement et modelisation en element fini *Setec Report* 2010

[7] C.-L. Lee, F.C. Filippou, Frame elements with mixed formulation for singular section response. *International Journal for Numerical Methods in Engineering* **78**, 1320-1344, 2009.

[8] S. Mohr, J.M. Bairan, A. R. Mari, A frame element model for the analysis of reinforced concrete structures under shear and bending. *Engineering Structures* **12**, 3936–3954, 2010.

[9] A. Papachristidis, M. Fragiadakis, Manolis Papadrakakis, A 3D fibre beam-column element with shear modelling for the inelastic analysis of steel structures. *Computational Mechanics* **6**, 553–572, 2010.

[10] A. Saritas, Mixed formulation frame element for shear critical steel and reinforced concrete members. *PhD thesis* University of California, Berkeley, 2006.

[11] R.L. Taylor, F.C. Filippou, A. Saritas, F. Auricchio, A mixed finite element method for beam and frame problems. *Computational Mechanics* **31**, 192–203, 2003.

[12] S.P. Timoshenko, J.M. Gere, Theory of Elastic Stability. *McGraw-Hill New York* 1961

[13] S. Zhou, Finite Beam Element Considering Shear-Lag Effect in Box Girder. *Journal of Engineering Mechanics* **136**, 1115–1122, 2010